AUSTRALIAN VETERINARY JOURNAL
AUSTRALIA'S PREMIER VETERINARY SCIENCE TEXT
WILDLIFE & ZOOS

CASE REPORT

Anaplastic thyroid carcinoma in a brush-tailed rock-wallaby (*Petrogale penicillata*)

RJT Doneley[a]* and WW Suen[b]

Background Neoplasia is considered to be rare in macropods. Anaplastic thyroid carcinoma (ATC) also known as undifferentiated or giant cell carcinoma, is a rare but aggressive and lethal solid tumour reported to affect humans, dogs, cats, racoons and birds. It is derived from poorly differentiated follicular cells and lacks the characteristic architectural pattern of arrangement of tumour cells. ATC has not previously been reported in macropods.

Case Report A brush-tailed rock-wallaby (*Petrogale penicillata*) was presented for a mass on the ventral neck. A clinical diagnosis of thyroid carcinoma was suspected based on radiology, ultrasound and cytology. Other than palliative care, treatment was declined. Four months later the wallaby was found dead and submitted for necropsy. Gross examination and histopathology demonstrated a unilateral ATC with vascular neoplastic emboli and distant metastases to the heart, lungs and liver.

Conclusion The clinical signs associated with thyroid tumours may be the result of localised growth and expansion of the thyroid, metastatic disease or a combination of these effects. Most thyroid tumours are nonfunctional. Based on the lack of typical clinical signs associated with functional thyroid tumours, in this case, we conclude that the thyroid tumour in this wallaby was likely to be nonfunctional. The cause of death in this wallaby was likely due to the heavy tumour burden with compromised cardiorespiratory function exacerbated by dorsoventral compression of the larynx. More study is needed to better understand thyroid neoplasia in macropods.

Keywords anaplastic; carcinoma; macropod; neoplasia; thyroid

Abbreviations ATC, anaplastic thyroid carcinoma; FNAB, fine needle aspirate biopsy

Aust Vet J 2022;100:271–276 doi: 10.1111/avj.13157

Usually originating from the follicular epithelium, thyroid tumours are histologically grouped into follicular, papillary, solid and anaplastic carcinomas.[1] All the subtypes of thyroid carcinoma can progress to anaplastic carcinomas, but papillary and follicular carcinoma are the most common types to undergo this transformation.[2] Papillary carcinomas are more common in humans than animals, and are predominantly well-differentiated thyroid carcinomas.[3] In dogs, thyroid tumours are usually follicular solid carcinomas and adenocarcinomas.[1] In one study in dogs, the incidence was reported to be 1.1% of all neoplasia seen.[4]

Anaplastic thyroid carcinoma (ATC), also known as undifferentiated or giant cell carcinoma[5] is one of the most aggressive and lethal solid tumours known to affect humans. It is derived from poorly differentiated follicular cells. The anaplastic tumour cells are large, pleomorphic and often spindle-shaped, making differentiation from a fibrosarcoma difficult. They lack a characteristic architectural pattern of arrangement of tumour cells. ATC is considered rare in humans,[3,4] dogs,[6] cats,[7] racoons[8] and birds.[9]

Neoplasia in macropods is uncommon; in one review of an Australian wildlife pathology register, only 14 cases of neoplasia were found in 444 macropods (3%), and none of them involved the thyroid gland.[10] This paper reports an ATC in a brush-tailed rock-wallaby (*Petrogale penicillata*), the first known report of this neoplasm in a macropod.

Case report

The patient was an 11-year-old, desexed male brush-tailed rock-wallaby (*P. penicillata*), presented to the University of Queensland Veterinary Teaching Hospital. It was a zoo animal, maintained in an outdoor enclosure with another wallaby, and fed a diet of commercial macropod pellets, poultry pellets, lucerne hay, vegetables (sweet potato and carrot).

The wallaby was presented with a 6-month history of a swelling on the left side of the neck. Since the animal had been difficult to handle on a regular basis, the keepers were unsure whether the swelling was present until it was large enough to be seen on distant examination. There were no reported changes in appetite or thirst, and no evidence of respiratory distress.

Physical examination under sedation (midazolam 1 mg/kg IM) revealed that the animal was in reasonable body condition, weighing 5.7 kg (normal weight for this species is 5.5–10.9 kg[11]). No abnormalities were detected other than a firm, nonmobile mass midway on the left side of the neck, measuring approximately 5 cm × 5 cm × 3 cm. It was considered too caudal to be considered an enlarged lymph node. There was no evidence of dental or mandibular disease.

The patient was anaesthetised (isoflurane by mask induction and maintenance) and ultrasound was performed of the mass (Figure 1).

*Corresponding author.
[a]School of Veterinary Science, The University of Queensland, Gatton, Queensland, Australia; r.doneley@uq.edu.au
[b]Australian Centre for Disease Preparedness (ACDP), Commonwealth Scientific and Industrial Research Organisation (CSIRO), East Geelong, Victoria, Australia

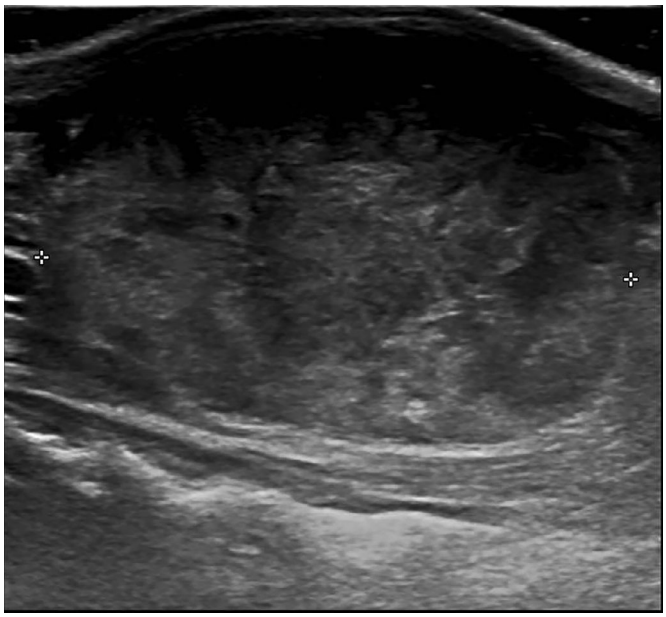

Figure 1. Ultrasound image of the mass (sagittal view).

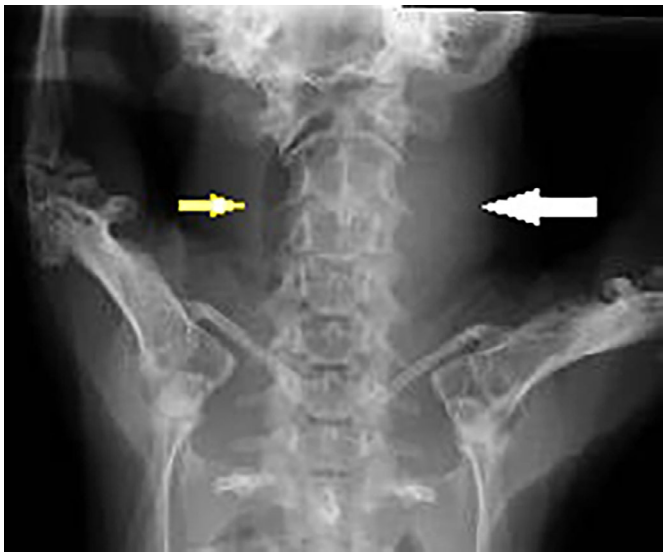

Figure 2. Radiograph of the dorsoventral view of the patient's thorax.

At the ventral aspect of the trachea (approximately 2–3 cm distal to the larynx) was a large heterogeneous, highly vascular, irregular, smoothly marginated mass (measuring 3 × 2.5 × 3.5 cm) with some mineralisation within the centre. This mass was believed to be a thyroid gland. The jugular veins were not included in the mass. The common carotid artery was closely abutting the mass but had a clear separate wall to the mass. There was no evidence of thrombus formation or vascular invasion. The contralateral thyroid was not identified.

Three radiographic views of the thorax (left and right laterals, and a dorsoventral view) were examined. The caudodorsal lung fields were diffusely opacified. The mainstem bronchi and vasculature were still visible. There was no evidence of nodules or masses in the thorax nor fascial planes cranially. The abdomen and musculoskeletal system appeared normal. A ventral mid-cervical soft tissue mass was present, containing some wispy mineralisation, displacing the trachea laterally. (Figure 2) The radiographic and sonographic diagnosis was a likely thyroid mass with no evidence of metastasis.

Multiple ultrasound-guided fine needle aspirate biopsies (FNABs) were collected from the mass and submitted for cytology. The biopsies contained few minimally pleomorphic epithelial cells and moderate to many moderately pleomorphic spindle cells present amid a background containing abundant blood with proportional leucocytes and platelet clumps. No microorganisms or inflammatory cells were noted.

The spindle cells were moderately pleomorphic, fusiform to less commonly oval, large (15–20 µm in diameter and up to 50 µm in length) and were present as both individualised and in small to occasionally very large clusters (Figure 3A). The nuclei were oval and centrally located with moderately stippled chromatin and often one, large prominent nucleolus (Figure 3A). The cytoplasm was moderately to deeply basophilic, moderate in amount, and occasionally vacuolated (Figure 3A). The pleomorphism was characterised by large size, moderate anisocytosis, moderate anisokaryosis, large prominent nucleolus and very rare binucleation.

The epithelial cells were minimally pleomorphic, cuboidal in shape and present in both individualised and small aggregates with distinct intercellular borders (Figure 3B). The nuclei were round and eccentrically located with moderately clumped chromatin and no visible nucleoli (Figure 3B). The cytoplasm was lightly basophilic and scant in amount (Figure 3B). Pleomorphism, when present, was characterised by marginal anisocytosis and anisokaryosis.

The high number and pleomorphism/atypia of the predominant cell population of spindle cells suggested a neoplastic proliferation. However, a definitive diagnosis could not be reached based on cytology alone, and differentials considered included a carcinoma with secondary reactive fibroplasia, a sarcoma arising within the thyroid gland, an atypical carcinoma, soft tissue sarcoma, haemangiosarcoma and marked reactive fibroplasia surrounding a benign epithelial lesion. We also considered an inadvertent aspiration of normal epithelial structures during the aspiration of the sarcoma.

The patient recovered uneventfully from the anaesthesia and was discharged. Further diagnostic testing and treatment (surgical resection) were discussed with the keepers but, in light of the wallaby's age and apparent good health, as well as the practical difficulties of administering and monitoring medication, further diagnostics and treatment were declined.

Two months later the wallaby was presented for reassessment. A small amount of weight loss was noted, and the animal appeared to be having difficulty eating grass, as it was seen to be eating from the side of the mouth. Tramadol (Tramal Oral Drops, Grünenthal GmbH, Germany), at 5 mg/kg q12h PO, was dispensed for palliative analgesia.

Four months after the initial presentation, the wallaby was found dead in its enclosure and submitted for necropsy. Its body condition was poor, with a prominent spine and pelvic bones.

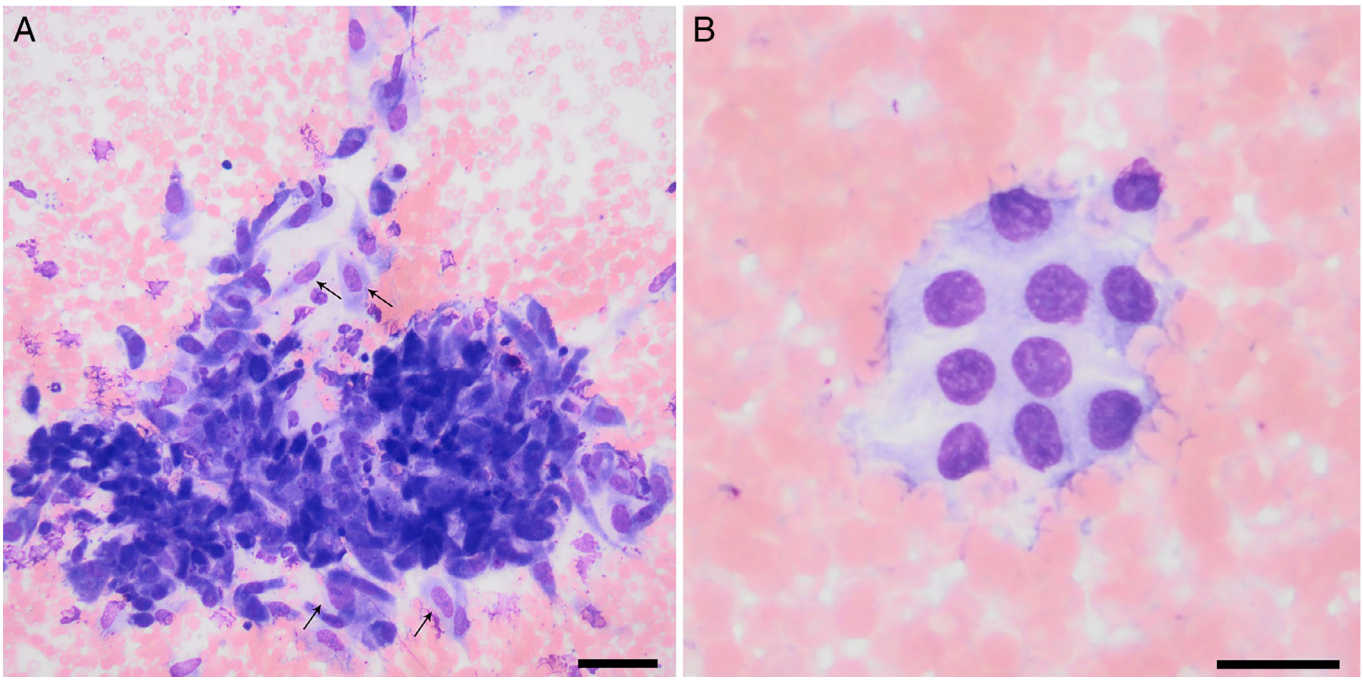

Figure 3. Aspirate of ventral neck mass. (A) The spindle cell population with moderate pleomorphism, oval centrally located nuclei containing stippled chromatin and often one prominent nucleolus (arrows). (B) The minimally pleomorphic epithelial cell population. Wright-Giemsa stain. Scale bar in (A) represents 50 µm and that in (B) represents 20 µm.

Figure 4. Ventral neck. On cut section, the ventral neck mass was solid and pale yellow with irregular multifocal to coalescing light yellow to white foci (arrows).

In the neck, a 4.5 cm × 4.5 cm × 5 cm, firmly attached, moderately well-demarcated, dark red mass was present. On cut section, the interior of the mass was solid and pale yellow with irregular multifocal to coalescing light yellow to white foci (Figure 4). Serial transverse sections revealed that the mass was arising from the right thyroid gland, expanding the subcutaneous tissue surrounding the lateral and ventral aspect of the larynx and compressing the larynx and cranial trachea dorsoventrally, reducing the lumen to 60% of the normal height. Regionally protruding from the ventral mucosa of the cranial trachea was a 3–5 mm diameter irregular nodule of similar consistency as the tumour (the histopathology of this is shown in Figure 5). This was interpreted as tumour invasion into the tracheal mucosa.

Affecting approximately 20% of all lung lobes were 20–50 small (5 mm diameter) beige to white round foci (Figure 6). The remaining lung was atelectatic and congested. Similar foci were present in all liver lobes (Figure 6). Focally expanding the endocardial surface and subendocardial myocardium of the right ventricular free wall near the papillary muscle was a 2 mm diameter beige round nodule. A larger soft nodule was adhered to the right atrial wall, occupying approximately 80% of the right atrial chamber.

Histopathology of the thyroid mass demonstrated a densely cellular, poorly demarcated and highly infiltrative neoplasm expanding out from the right thyroid gland, invading out of the thyroid capsule and compressing the larynx and trachea dorsoventrally. This mass was composed of three cell phenotypes: polygonal cells were arranged in either follicles (follicular cell morphology; Figure 7) or ill-defined packets (compact cellular morphology; Figure 7); and plump-spindloid to pleomorphic anaplastic cells arranged in streams and sheets (giant cell morphology; Figure 8). In this pleomorphic cell population, anisocytosis and anisokaryosis were more prominent than those seen in the other two cell phenotypes. This was accompanied by occasional multinucleation (often binucleation), karyomegaly (Figure 8) and rare, bizarre mitotic figures. Frequent small areas of necrosis (Figure 8) and neoplastic vascular emboli were present in the tumour, particularly in the giant cell region.

Figure 5. Transverse section of the trachea showing the highly infiltrative thyroid carcinoma (TC) invading the ventral tracheal submucosa forming a plaque (arrows) that protruded into the tracheal lumen (L). For orientation, the letter C denotes the tracheal cartilage. H&E stain. ×0.7 magnification. Scale bar represents 2 mm.

Figure 6. Lung lobes contain multiple firm, beige to white, round metastatic nodules (arrows). The liver also contains a couple of similar metastatic foci (arrowheads).

Separating the neoplastic cells was low to moderate amount of collagenous matrix interpreted as scirrhous reaction. Scattered throughout the neoplasm were moderate numbers of individual neutrophils and aggregates of plasma cells, lymphocytes and macrophages. Of the three morphologic patterns, the giant cell morphology predominated the tumour, in particular, in distant areas away from where the original thyroid gland was expected to be. This was suggestive of increased clonal malignancy in distant neoplastic cell populations.

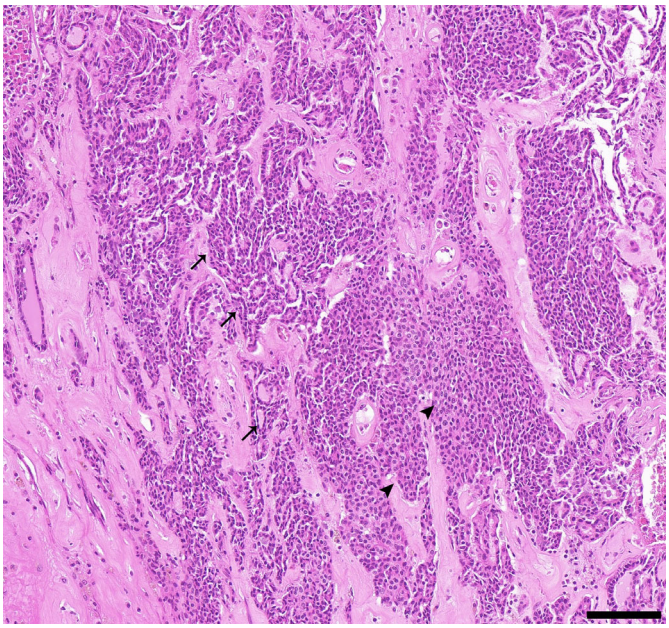

Figure 7. Polygonal neoplastic cells were arranged in follicles (follicular pattern, arrows) and ill-defined solid packets (compact cellular pattern, arrowheads). H&E stain. ×20 magnification. Scale bar represents 100 µm.

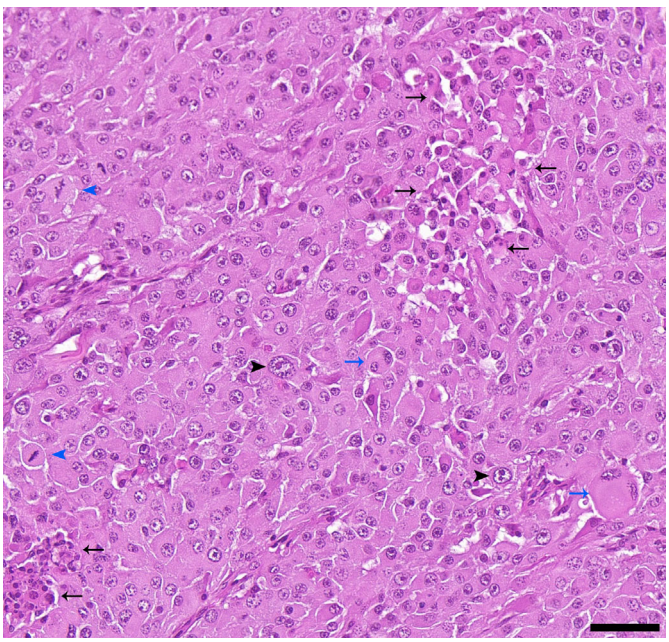

Figure 8. Neoplastic cells were also spindloid to pleomorphic arranged in sheets, interspersed with necrotic foci (demarcated by black arrows), karyomegalic (black arrowheads) and multinucleated cells (blue arrows). In this view, there are also a few mitotic figures (blue arrowheads). H&E stain. ×36.5 magnification. Scale bar represents 50 µm.

Regionally effacing and breaching a 3 mm wide stretch of the ventral tracheal mucosa were infiltrating packets of neoplastic cells projecting a 4 × 1.5 mm plaque into the lumen (Figure 5). Elsewhere, laryngeal and tracheal submucosa contained mixed leucocytes, consisting of

neutrophils, lymphocytes and macrophages. The laryngeal and tracheal epithelium was diffusely lined by tall hyperplastic epithelial cells.

Affecting all lung lobes and expanding a third of the pulmonary interstitium with perivascular distribution were similar nests and packets of neoplastic cells of mostly the giant cell morphology as described above. Neoplastic cells also breached the pleura in multifocal patches. Similar neoplastic cells were present in a small nodule in the subendocardial myocardium of the right ventricular free wall. Myocardial fibrosis and compensatory hypertrophy were present in the left ventricular myocardium.

Metastatic nodules with mostly the giant cell morphology as described above were present in the liver and neoplastic infiltrates were present in many of the regional lymph nodes. In general, as compared to the primary tumour, the metastatic nodules appeared to contain more multinucleated and karyomegalic cells, as well as bizarre mitotic figures. No metastases were identified in the gastrointestinal tract, kidneys, spleen or brain.

The final diagnosis was a unilateral ATC with vascular neoplastic emboli and distant metastases to the heart, lungs and liver. The cause of death was likely due to the heavy tumour burden in this animal with compromised cardiorespiratory function exacerbated by dorsoventral compression of the larynx. The left myocardial fibrosis could have been secondary to a chronic infarct from vascular neoplastic embolus and may have contributed to the patient's death.

Discussion

The clinical signs associated with thyroid tumours may be the result of localised growth and expansion of the thyroid, metastatic disease or a combination of these effects.

In dogs most thyroid tumours are nonfunctional, benign adenomas; hyperthyroidism is rare and usually mild as dogs have a much more efficient enterohepatic excretory mechanism for thyroid hormones than cats.[13] In cats, hyperthyroidism is usually associated with functional thyroid hyperplasia and follicular cell adenomas,[13] while malignant carcinomas are the least common cause of hyperthyroidism (1%–3% of thyrotoxic cats).[1]

However, thyroid carcinomas often grow rapidly, invading adjacent structures, such as the trachea, oesophagus and larynx, and are usually fixed in position. The earliest and most frequent site of metastasis is the lung, because thyroid carcinomas tend to invade branches of the thyroid vein.[12] ATC is considered rare in most animal species.[7–10] It is also considered rare in people and has a high mortality rate.[3,4] This mortality is associated most commonly with asphyxia due to tracheal compression, but local and distant metastatic disease is common. Are and Shaha[3] reported that metastatic disease is seen in 50% of human patients at presentation, and another 25% develop metastasis during the illness. The lung is the most common site (80%), followed by bone (6%–15%) and brain (5%–13%). Rarely, cardiac and intra-abdominal metastasis have also been reported.[4]

Medical literature, although limited, reports that FNAB of ATC appears to have high sensitivity and specificity, detecting 80%–90% of cases (misdiagnosis is associated with inadequate sampling). However, the diagnosis of ATC can be challenging because of the variable appearance of aspirated cells and a broad differential diagnosis that includes medullary carcinoma, poorly differentiated thyroid carcinoma, lymphoma, primary thyroid sarcoma and metastatic tumours. Although ATC arises in many cases from a well-differentiated thyroid carcinoma, the limited nature of an FNAB specimen usually precludes identification of an associated lower-grade lesion.[13]

Surgical biopsy, either incisional or excisional, appears to offer the most definitive antemortem diagnosis of ATC. There are three main histological patterns, often coexisting: spindle cell, pleomorphic (giant cell) and squamoid. The spindle cell pattern resembles a high-grade sarcoma in most cases, with significant pleomorphism, cellularity and necrosis. The squamoid pattern is composed of sheets of epithelioid malignant cells with abundant dense eosinophilic cytoplasm and rarely overt keratin production. The pleomorphic pattern consists of highly pleomorphic round to polygonal cells and frequent giant cells. Giant cells can take the form of large bizarre, pleomorphic tumour giant cells, multinucleated foreign body giant cells or osteoclast-type multinucleated giant cells.[5] Necrosis and haemorrhage are common in ATC and can be extensive.[12,13]

The thyroid glands in macropods are located on the anterolateral side of the neck at a level between the larynx and trachea. They are composed of bilaterally separated long lobes, rarely linked ventrally by a thin isthmus.[14,15] ATC has not been previously reported in macropods.[10] In this case, the primary tumour had locally infiltrated into the tracheal lumen and had metastasised to the heart, lungs and liver, behaving similarly to the disease in humans. Based on the lack of clinical signs on initial presentation in this case, the ATC may be nonfunctional and exerts its effects on the animal by compression of surrounding tissue and heavy tumour burden due to metastatic disease. The emaciated state of this animal at the time of death is likely a reflection of the heavy tumour burden, and this aligns with what has been described in humans with ATC, where dysphagia and dyspnoea associated with thyroid enlargement are common symptoms.[3,5] Further observations of this disease in macropods are necessary to draw more conclusive opinions on the biological behaviour of this tumour.

Acknowledgments

We would like to thank Dr Karen Jackson, Dr Rachel Allavena and Dr Mainity Batista Linhares for their input and assistance with this case. Open access publishing facilitated by The University of Queensland, as part of the Wiley – The University of Queensland agreement via the Council of Australian University Librarians.

Conflicts of interest and sources of funding

The authors declare no conflicts of interest or sources of funding for the work presented here.

References

1. Kessler M. Surgery in thyroid disease. *Proceedings of the annual conference of the World Small Animal Veterinary Association*, 2014. Available at: https://www.vin.com/members/cms/project/defaultadv1.aspx?id=7054770&pid=12886&. Accessed 24 December 2021.
2. Swami SY, Chopwad AD, Valand AG. Undifferentiated/anaplastic thyroid carcinoma: A cytological case report. *Med J DY Patil Vidyapeeth* 2018;11:449–451.

3. Are C, Shaha AR. Anaplastic thyroid carcinoma: Biology, pathogenesis, prognostic factors, and treatment approaches. *Ann Surg Oncol* 2006;13:453–464.
4. Wucherer KL, Wilke V. Thyroid cancer in dogs: An update based on 638 cases (1995-2005). *J Am Anim Hosp Assoc.* 2010;46:249–254.
5. Ragazzi M, Ciarrocchi A, Sancisi V et al. Update on anaplastic thyroid carcinoma: Morphological, molecular, and genetic features of the most aggressive thyroid cancer. *Int J Endocrinol* 2014;2014:790834.
6. Firmo BF, Lobo CPC, Siquiera RC et al. Thyroid Gland Carcinoma in 11 Dogs: A Retrospective Study. In: Veterinary Cancer Society Conference 2016 World Congress.
7. Patnaik AK, Lieberman PH. Feline anaplastic giant cell adenocarcinoma of the thyroid. *Vet Pathol.* 1979;16:687–692.
8. McCain SL, Allender MC, Bohling M et al. Thyroid neoplasia in captive raccoons (*Procyon lotor*). *J Zoo Wildl Med.* 2010;41:121–127.
9. Bates G, Tucker RL, Ford S et al. Thyroid adenocarcinoma in a bald eagle (Haliaeetus leukocephalus). *J Zoo Wildl Med.* 1999;30:439–442.
10. Canfield PJ, Hartley WJ, Reddacliff GL. Spontaneous proliferations in Australian marsupials—a survey and review. 1. Macropods, koalas, wombats, possums and gliders. *J Comp Pathol* 1990;103:135–146.
11. *Petrogale penicillata*—brush-tailed rock wallaby: Species profile and threats. Australian Government Department of Agriculture, Water and Environment. Available at: http://www.environment.gov.au/cgi-bin/sprat/public/publicspecies.pl?taxon_id=225. Accessed 13 March 2020.
12. Rosal TJ, Grone A. Endocrine glands. In: Maxie MG, editor. *Jubb, Kennedy, and Palmer's pathology of domestic animals*. 6th edn. Vol. 3. Elsevier, St. Louis, MO, 2016;269–357.
13. Goicochea L, Staats P. Anaplastic thyroid carcinoma, a cytologic perspective. *Pathol Case Rev* 2015;20:214–217. https://doi.org/10.1097/PCR.0000000000000107.
14. Yamasaki M. Comparative anatomical studies on the thyroid and thymic arteries. VI. *Diprotodont marsupials*. *Anat Sci Int* 2016;91:258–273.
15. Dawson TJ, Finch E, Freedman L et al. Morphology and physiology of the Metatheria. In: *Fauna of Australia volume 1b Mammalia*. Australian Government Publishing Service, Canberra, 2020. Available at: https://www.environment.gov.au/system/files/pages/a117ced5-9a94-4586-afdb-1f333618e1e3/files/17-ind.pdf. Accessed 12 March 2020.

(Accepted for publication 21 February 2022)